A GPR System Using a Broadband Passive Optical Sensor for Land Mine Detection

Ryohei Tanaka, Motoyuki Sato
Center for Northeast Asian Studies, Tohoku University
Sendai, 980-8576, Japan
rtanaka@cneas.tohoku.ac.jp sato@cneas.tohoku.ac.jp

***Abstract*—A new GPR system, which uses an optical electric field sensor, was discussed. We proposed a new bistatic radar system, which is consisted of a TEM horn antenna as a transmitter and an optical sensor as a receiver. A broadband type optical sensor with a frequency bandwidth from 100MHz to 5GHz was applied to the land mine detection. Laboratory measurements showed that buried objects can be detected by the new GPR system. We found the difference of the reconstructed image dependent on the incident wave polarization.**

Keywords:Bistatic radar, GPR, landmine detection, Optical electric field sensor, polarization

I. INTRODUCTION

Over 10 million land mines are still remained all over the world and it might take more than one thousand years to remove all land mines due to the conventional method of demining. The Japanese government officially stated necessity of the recovery of Afghanistan, which is suffered from land mine harm and asked universities to develop humanitarian demining techniques. Our research group has developed various land mine detection techniques [1]. And up to now, an optical sensor, whose higher frequency is up to 1 GHz, has been used [2]. In this paper, we will present a new GPR system using a broadband passive optical electric field sensor having a bandwidth from 100MHz to 5GHz as a receiver. Then discuss on the improved imaging techniques.

II. OPTICAL ELECTRIC FIELD SENSOR FOR GPR

In this section, we introduce the basic principle of the optical electric field sensor and the developed passive optical sensor for a GPR system [3]. Fig. 1 shows the optical electric field sensor attached on a scanning arm. Fig. 2 shows the construction of the optical electric filed sensor. Optical wave guides are cut on $LiNbO_3$ wafer and it branches off. The electric field through electrodes affects one branched optical guide, and the other is not affected. The electric field modulates the refraction ratio of the optical guide, and the phase of light, which propagates through this guide, is modulated. As a result, when those two optical signals are combined, the amplitude of the input signal is modulated due to the interferometric effect.

The optical electric field sensor has several advantages. Firstly, because it modulates the optical signal strength by the electric field strength, the sensor does not need a metal coaxial cable, which disturbs the electric field. Secondly, the sensor itself is consisted of nonmetallic parts except electrode and antenna element. Thus little disturbance toward electric field is expected. Thirdly, the size of the sensor is small (1cm x 7cm). This makes possible to scan in a narrow space or near the ground surface.

Fig. 3 shows the measurement system using a double-ridged horn antenna (ETS Model 3106) as a transmitter and the optical sensor (TOKIN) as a receiver. Laser as a source is put into the sensor, and the modulated signal is detected by an optical detector. A vector network analyzer (HP8753E) is connected to the optical detector and the horn antenna by coaxial cables and transmits and receives signals in frequency domain. And the system is operated as stepped frequency radar.

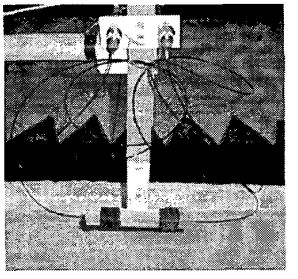

Figure 1. Optical electric field sensor on a scanning arm.

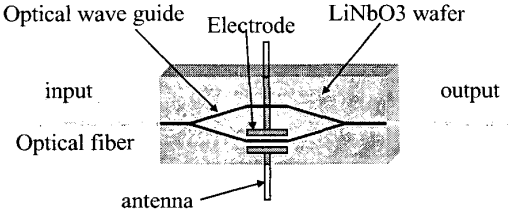

Figure 2. Construction of the Optical electric field sensor.

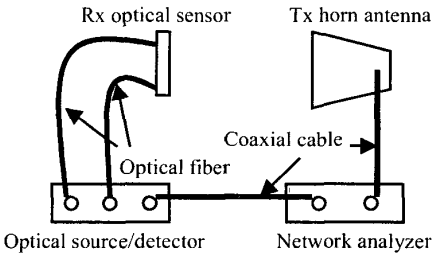

Figure 3. Measurement system diagram using an optical electric field sensor.

III. LABORATORY EXPERIMENT

Bistatic radar system is useful to reduce the influence of the reflection wave from the ground surface. Also, the small size of the optical sensor gives effective scanning on the irregular ground surface.

Figs.4 and 5 show the configuration of the transmitter and the receiver with a target in air and a buried target respectively. The transmitter is fixed at a position and the receiver scans horizontally on the target. When the target is in the air, the area of scanning is 80cm x 84cm and the height of the sensor is 14.5cm. When the target is buried in dry sand with the permittivity of 2.5, the area of scanning is 52cm x 75cm, the height of the sensor is 11.5cm and the transmitter angle is set at 30 degrees downward the sand surface. In the former case, the target is a metallic sphere having a diameter of 75mm and in the latter case, the target is a sphere having a diameter of 75mm covered with aluminum foil buried at 5 cm in depth. All the measurements were carried out in an anechoic chamber. In both cases, the increment of the scanning is 1 cm and the target is located at the center of the scanning area.

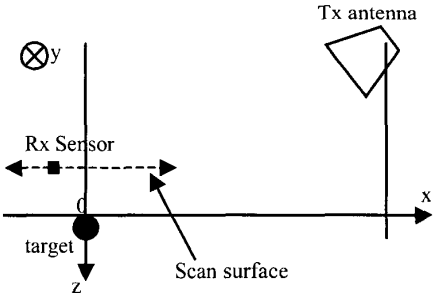

Figure 4. Configuration of measurement with a target.

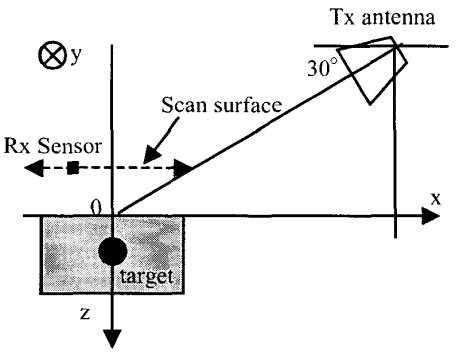

Figure 5. Configuration of measurement with a buried target.

In these measurements, two incident polarizations, namely vertical(TM mode) and horizontal (TE mode) were applied. Fig. 6 shows the unburied target detection with TM polarization incidence and Fig .7 shows buried target detection with TE polarization. When the target is buried, EM absorber was attached at the side of the sand box to reduce the reflected wave from the wall of the box. Frequency domain data were acquired from 50MHz up to 5GHz at 401 frequency points.

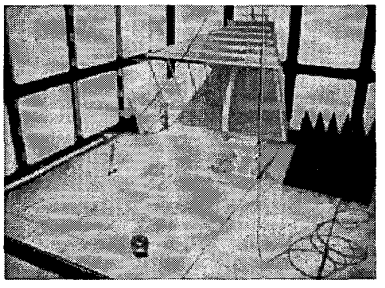

Figure 6. Target detection by TM mode incidence.

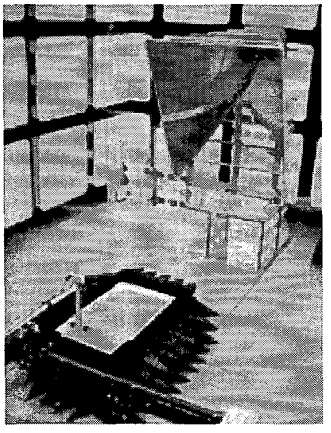

Figure 7. Buried target detection by TE mode incidence.

IV. IMAGING RECONSTRUCTION

The acquired data were transformed into time domain data by FFT and SAR processing was carried out. We used inverse filtering before SAR processing to compress direct wave. Inverse filtering is shown in (1).

$$f'(t) = \mathbb{F}^{-1}\left[B(\omega)\left(F(\omega)/F_{ref}(\omega)\right)\right] \quad (1)$$

In (1), $\mathbb{F}^{-1}$ is inverse Fourier transformation, $B(\omega)$ is a band pass filter and F_{ref} is the reference signal, and we used a direct wave for F_{ref}. SAR processing of diffraction stacking algorithm is shown as in (2).

$$S_{m,n,o} = \sum_{i,j} A_{i,j}(t - \tau_{i,j,m,n,o}) \quad (2)$$

In (2), $A_{i,j}$ is amplitude, $\tau_{i,j,m,n,o}$ is the travel time along a path from the transmitter to the receiver via imaging grids when the receiver is at the *i*-th and *j*-th position and the imaging grid is at the *m*-th, *n*-th and *o*-th.

For the buried target case, SAR processing was implemented with two layers model. It is assumed that the energy impinges on the ground surface right above the target and then reaches to the target vertically. The travel path from the target to the receiver is the same process as the path from the transmitter to the target.

Figs. 8 and 9 show the migrated images of the target in air with TE and TM mode. The parameter z indicates a horizontal slice by diffraction stacking and the negative value means that the slice is above the top of the target. From the results, the target is detected clearly in TE and TM cases. For the target in air, similar imaging results between TE and TM mode were expected, and this phenomenon can be seen from the results. And, we can conclude that the optical electric field sensor has a higher ability than the former narrowband type optical sensor [2].

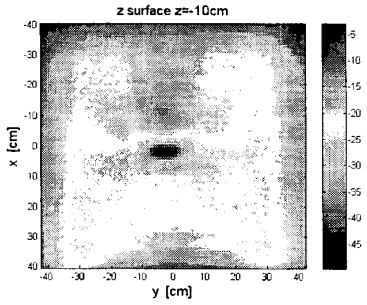

(b) z=-10cm.

Figure 8. Reconstructed image of a target in air by TE mode.

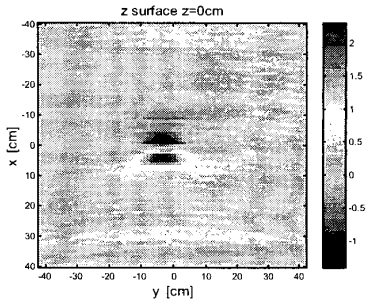

z=0cm.

Figure 9. Reconstructed image of a target in air by TM mode.

Figs. 10 and 11 show migrated results of the buried target for TE and TM mode measurement respectively. In Figs. 10(b) and 11(b), the target is detected at the center of the scanning area.

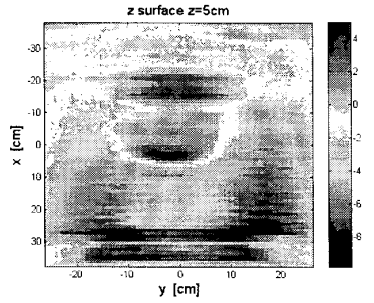

(a) z=5cm.

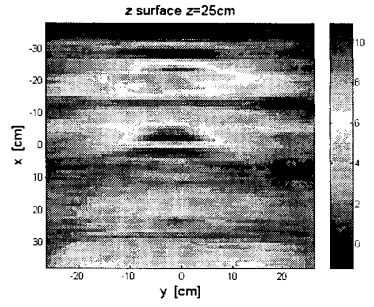

(b) z=25cm.

Figure 10. Reconstructed image of a buried target by TE mode.

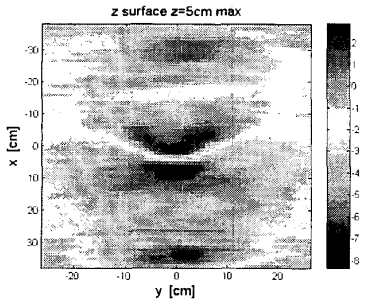

(a) z=5cm.

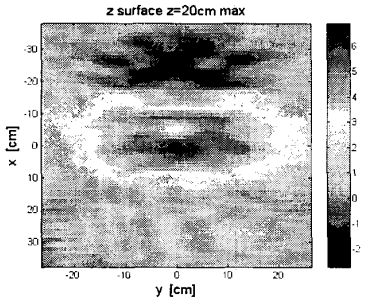

(b) z=20cm.

Figure 11. Reconstructed image of a buried target by TM mode.

V. DISCUSSION

In Fig. 10(a) and Fig. 11(a), when the imaging depth is at the real position of the target, the target is not clearly imaged like the target in air. This might be due to the process of inverse filtering. On inverse filtering, time shift caused by division is compensated, and we estimated the time shift from the reference signal manually. This procedure can cause error. In addition, an incorrect permittivity of sand could cause fuzzy images as in Figs. 10 and 11. To reduce the reflection wave from the ground surface, the effect of the Brewster angle has been clarified at our laboratory [2]. And this time, we also tried to take the advantage of the Brewster angle in TM mode measurement. In TM mode measurement, theoretically weak reflection from the ground surface occurs and as a result, the reflection signal from the target will be emphasized. However, comparing Fig. 10 and Fig. 11, we cannot observe the obvious effect of the Brewster angle. In the buried target measurement, the sand box was not large enough (55cm x 32cm), thus reflection wave from the edge or the bottom of the sand box could be obstruction to the clear imaging and the effect of the Brewster angle. Also, the edge of the sand box could cause the bright area at x = -20cm in Fig. 10 and 11. So, the target will be imaged clearer if we use large enough sand box. In addition, the optical sensor itself might work similar to a dipole antenna. In TE mode measurement, the sensor was put in perpendicular to x-axis, on the contrary, in TM mode measurement, the sensor was put in parallel to x-axis, which possibly weakened the Brewster angle effect relatively.

VI. CONCLUSION

We showed experiment results of a bistatic radar system using a broadband type optical electric field sensor. The optical sensor could detect the unburied target clearly. Also for the buried target, the sensor system could detect the target too. Hence, the target detection ability of the proposed system could be demonstrated. But the imaging results, especially at buried cases, were not clear enough due to the error in inverse filtering and the accuracy of the permittivity. As the future work, we are planning to perform the same measurement at a large sand pit instead of at an anechoic chamber and design suitable antenna elements to be attached on the optical sensor to increase gain.

VII. ACKNOWLEDGMENT

This work was supported by JSPS Grant-in-Aid for Scientific Research (s) 14102024.

VIII. REFERENCES

[1] M. Sato, Yusuke Hamada, Xuan Feng, Fan-Nian Kong, Zhaofa Zeng and Guangyou Fang, "GPR using an array antenna for landmine detection," Near Surface Goephysics, 2004, pp. 3-9

[2] M. Sato, "A new bistatic GPR system using apassive optical sensor for landmine detection," Proceedings of the 2nd International Workshop on Advanced Ground Penetration Radar, Delft, The Netherlands, May 2003, pp. 164–167.

[3] N. Kuwabara, K. Tajima, R. Kobayashi and F. Amemiya, "Development and analysis of electric field sensor using LiNbO3 optical modulator," *IEEE Trans.* Electromagnetic Comp., vol.34, no.4, Nov.1992.